Application of Crescent-Shaped Brace passive resisting system in RC frame structures

Application of Crescent-Shaped Brace passive resisting system in multi-storey frame structures

Omar Kammouh[1], Stefano Silvestri[2], Michele Palermo[3], Gian Paolo Cimellaro[4]*,

[1, 4]*Politecnico di Torino*

[2,3]*University of Bologna*

ABSTRACT

The design of building structures that is capable of providing prescribed seismic performances is the fundamental objective of the Performance-Based Seismic Design (PBSD) approach. Matching a particular seismic response requires additional design freedom that the conventional structural elements (beam/column) fail to provide. Here, it is worth to highlight the role of innovative lateral resisting systems such as base isolation and dissipative systems, which can add flexibility to the design and help to achieve prefixed seismic performance objectives. Among different solutions, the seismic design of a two-storey reinforced concrete building equipped with a novel hysteretic device, namely Crescent-Shaped Brace (CSB), is presented. CSBs are characterised by a unique geometrical configuration, leading to an optimized nonlinear force-displacement behaviour that allows the structure to achieve prescribed multiple seismic performances. In this paper, we propose a procedure for the seismic design of the CSB devices within the framework of PBSD. The global behaviour of the devices is studied and verified for a multi-storey shear-type building structure by means of numerical analyses. The results obtained confirm the validity of the proposed design method and the effectiveness of the new hysteretic device. The force-displacement curve of the building matches the objectives curve (i.e. the one corresponding to the predefined performance objectives), thus ensuring the fulfilment of the prescribed multi-seismic performances.

Keywords: *Crescent Shaped Brace, Design method, Dynamic analysis, Performance Based Seismic Design.*

1 INTRODUCTION

Advancement in earthquake engineering has recently led to the birth of new structural design philosophies, such as the Performance-Based Seismic Design (PBSD) [1]. Although it goes back to the late 20th century, PBSD is still considered recent because of its design efficiency [2]. Performance-Based Design indicates the primary objectives that should be achieved by the structure and gives the criteria for accepting a given performance [3]. Nowadays, buildings are designed and strengthened in order to fulfil the predefined performance levels indicated by the design codes because the challenge is no more limited to saving lives, but rather to minimising damage and functional disruption down to acceptable levels. However, matching a certain seismic response

[1] Ph.D. student, omar.kammouh@polito.it

[2] Associate professor, stefano.silvestri@unibo.it

[3] Research Scientist, michele.palermo7@unibo.it

[4] Associate professor, gianpaolo.cimellaro@polito.it

* Corresponding author

requires additional design freedom that the conventional structural elements (beam/column) are not capable to provide. Here, it is noteworthy to highlight the role of innovative lateral resisting systems which add flexibility to the design and help to achieve prefixed seismic performance objectives.

Recently, several attempts in the earthquake engineering field could find their ways into numerous innovative systems that provide the structure with a specific performance under a given earthquake level. Among others, the most known systems are: (a) seismic isolation systems, which uncouple the superstructure from its substructure leading to a "conceptual separation between the horizontal and vertical resisting systems" [4]; (b) tuned mass damping systems, which are used to minimize the excitation of a structure caused by high lateral vibrations [5]; (c) active and semi-active systems, which adjust the mechanical properties of a structure in accordance with the measured response [6]; (d) dissipative systems, which are inserted in the superstructure in order to minimize the seismic effects in the structure through their energy dissipation capacity [7]. Although the listed systems have been well integrated into literature and practice, none of them could entirely fulfil the seismic performance objectives of the structure.

In this paper, we focus on a novel lateral resisting device, namely the Crescent-Shaped brace (CSB). CSB is a hysteretic device that falls in the passive energy dissipation category, allowing the structure to have prescribed multiple seismic performances [8]. As of yet, the design of multi-storey building structure equipped with Crescent-Shaped Braces has not been exposed to extensive research. As far as the global behaviour of structures is concerned, up to now CSBs were only inserted at the ground floor of a steel structure in order to realize a controlled soft-storey response, while the upper storeys were braced with conventional concentric steel diagonal braces so that the structure could be conceptually modelled as a single degree of freedom (SDOF) system [4].

The presented work proposes an exhaustive procedure for the seismic design of a multi-storey shear-type frame structure equipped with the CSB devices. The proposed method can be applied to both single and multi-degree-of-freedom shear-type structures. To describe the procedure in all the details, a two-storey reinforced concrete case study structure is considered. The equipped structure is designed in such a way to meet the "Essential Objectives" indicated in Fig. 1 [1]. After the design, the performances of the equipped building under different seismic design levels are numerically obtained through non-linear time-history and pushover analyses. The results obtained in this paper confirm the validity of the proposed design method and the effectiveness of the new hysteretic device.

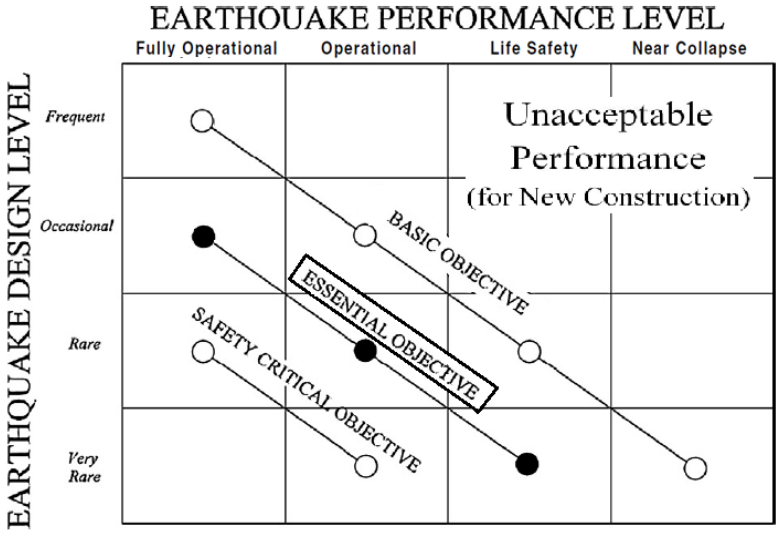

Figure 1- Performance-based seismic design objectives, adopted from [9]

2 THE CRESCENT-SHAPED BRACES

2.1 Overview

Crescent-Shaped brace (CSB) is a special lateral resisting device that is capable of providing additional design freedom to frame structures. Its geometrical configuration, as shown in Fig. 2, allows the structure to have prescribed multiple seismic performances within the performance-based design scheme [8]. The Crescent-Shaped Braces enable the designer to have control over the design because their strength at yielding is not coupled with their lateral stiffness.

2.2 Analytical model of the CSB

In their previous work on the Crescent-Shaped Braces, Palermo et al. (2014) have derived analytical formulas that allow sizing the device given its target stiffness and target yield strength. Equations (1) and (2) are simplified versions of the equations presented in Palermo et al. (2014). Stiffness and strength are initially imposed by the predefined performance objectives of the specific structure considering the structural and non-structural responses. Equation (1) allows obtaining the arm ratio of the device, which is the ratio between the arm of the device "d" and the diagonal length "L". The arm ratio is then substituted in Eq. (2) to obtain the moment of inertia of the CSB device. Full detail on the derivation of these equations can be found in [8].

$$\xi = \frac{M_{pl}}{\overline{F_y}.L}. \tag{1}$$

where $\xi = d/L$ is the arm ratio of the device (can be assumed 0.1 for preliminary design), d is arm of device arm, $M_{pl} = W_{pl} \cdot f_y$ is the plastic bending resisting moment of the cross section, W_{pl} is the plastic section modulus, f_y is the yield strength, $\overline{F_y}$ is the target yield strength, L is the diagonal length.

$$J = \frac{L^3 \cdot \overline{K} \cdot \xi^2}{3 \cdot E \cdot \cos^2 \theta}. \tag{2}$$

where J is the moment of inertia of the cross-section, $\overline{K}$ is the target initial lateral stiffness, E is the elastic modulus of the steel cross-section, θ is the angle between the force and the diagonal when the device is installed in a frame structure (in Fig. 2 $\theta = 0$).

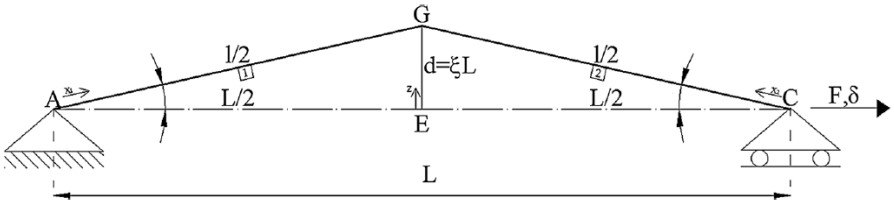

Figure 2- The geometric configuration of the studied device [8]

2.3 Mechanical behaviour of the CSB

The post-yielding behaviour of the bracing device is numerically studied using the fibre-based program 'SeismoStruct V.7.0.6' [10]. Seismostruct takes into account the geometric nonlinearity according to the corotational formulation [11], and the material non-linearity according to Menegotto-Pinto law, considering the isotropic hardening as given by [12].

A specimen of the bracing device (HE200B European profile) is firstly subjected to a monotonic increasing tension loading, and the result is reported in Fig. 3(a). The force-displacement behaviour of the device looks quite complex. In the first part of the curve, the CSB responds mainly in flexure and behaves linearly until it reaches the yielding at the knee section. Afterwards, the device experiences a softening behaviour at the plasticization of the knee section (pseudo-horizontal part), followed by a significant hardening behaviour as the device gets more and more elongated and thus responding mainly through its axial stiffness capacity, like a conventional brace or a truss in a tensile configuration.

Likewise, the same sample is subjected to monotonically increasing compressive loading, considering the geometrical and the mechanical nonlinearity of the device. The constitutive law of the hysteretic device in compression is given in Fig. 3(b). It is worth to note that unlike a conventional brace, the CSB device does not suffer from in-plane buckling or a sudden capacity drop because of its special geometrical configuration. Out-of-plane buckling should (and can easily [8]) be prevented by means of proper choice/design of the cross section (e.g. balanced inertias along strong and weak axes, or addition of longitudinal ribs in correspondence to the neutral axis fibre).

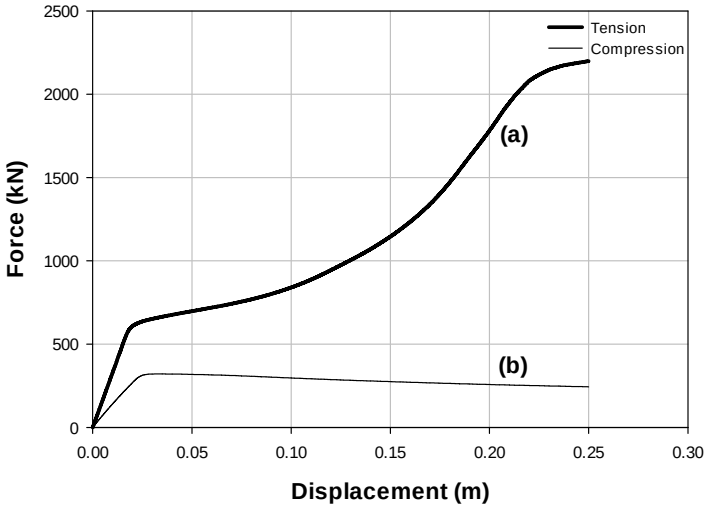

Figure 3- (a) Monotonic behavior of a single CSB in tension; (b) Monotonic behavior of a single CSB in compression

3 PERFORMANCE-BASED DESIGN OF A MULTI-STOREY SHEAR-TYPE FRAME EQUIPPED WITH CSB DEVICES

As a new system, the CSB still lacks a comprehensive seismic design procedure that can be followed regardless the structure's type. In the literature, the behaviour of an SDOF steel structure with this device being installed was investigated [4]. The design procedure used in that particular case, however, cannot be considered a reference point for other studies because it was built upon very specific structural conditions. In this section, we propose a more exhaustive procedure for the seismic design of a multi-storey shear-type frame equipped with Crescent-Shaped Braces (CSB) based on the modal analysis. The proposed method may be used to design or strengthen structural systems that do not satisfy particular pre-defined performance objectives.

The design procedure is illustrated in Fig. 4. The purpose of this design procedure is to obtain a target lateral stiffness for the single CSB device. The stiffness term is then used in the previously-delivered design formulas (Eqs. (1) and (2)) to get the inertia demand of the brace. Once securing the moment of inertia, the cross section profile of the device can be chosen accordingly. It is worth to note that the cross section choice controls the post yielding behaviour of the bracing device, which in turn affects the post yielding behaviour of the whole structure [8]. Without loss of

generality, in the following, a three-DOF system schematization is used to describe in details the steps of the design procedure.

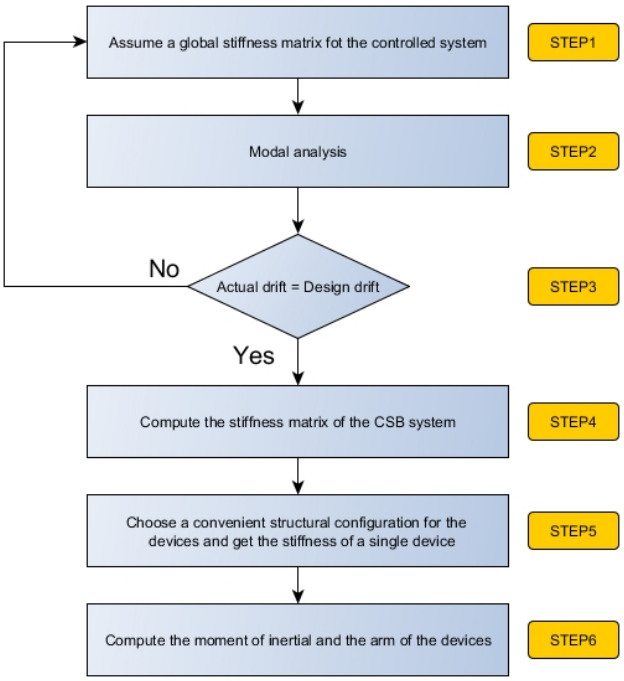

Figure 4- Flowchart of the CSB design scheme

3.1 Step 1: Global stiffness matrix

The global stiffness matrix describes the stiffness of the controlled system (i.e. bare structure + CSB devices). This matrix can be derived by combining (as they act in parallel) the stiffness matrices of both the uncontrolled system and the bracing system.

3.1.1 Stiffness matrix of the uncontrolled system

$$[K]=\begin{pmatrix} k_1+k_2 & -k_2 & 0 \\ -k_2 & k_2+k_3 & -k_3 \\ 0 & -k_3 & k_3 \end{pmatrix}. \tag{3}$$

where $[K]$ is the stiffness matrix of the uncontrolled system, k_1, k_2, and k_3 are the stiffness terms of the uncontrolled system at the first, second, and third storeys respectively. All matrix's components are known and can be derived by applying the direct stiffness method.

3.1.2 Stiffness matrix of the CSB system

$$[K_b]=\begin{pmatrix} k_{b1}+k_{b2} & -k_{b2} & 0 \\ -k_{b2} & k_{b2}+k_{b3} & -k_{b3} \\ 0 & -k_{b3} & k_{b3} \end{pmatrix}. \tag{4}$$

where $[K_b]$ is an unknown stiffness matrix belonging the bracing system, k_{b1}, k_{b2}, and k_{b3} are the stiffness terms of the braring system at the first, second, and third storeys respectively.

3.1.3 Global stiffness matrix of the controlled system (uncontrolled structure + CSB)

$$\left[K^*\right]=\left[K\right]+\left[K_b\right]=\begin{pmatrix} k_1^*+k_2^* & -k_2^* & 0 \\ -k_2^* & k_2^*+k_3^* & -k_3^* \\ 0 & -k_3^* & k_3^* \end{pmatrix}. \quad (5)$$

where $\left[K^*\right]$ is the stiffness matrix of the controlled system, k_1^*, k_2^*, and k_3^* are the stiffness terms of the controlled system at the first, second, and third storeys respectively, and they are given as follows:

$$\begin{aligned} k_1^* &= k_1 + k_{b1} \\ k_2^* &= k_2 + k_{b2} \\ k_3^* &= k_3 + k_{b3} \end{aligned} \quad (6)$$

3.1.4 Storey stiffness distribution

The global stiffness matrix $\left[K^*\right]$ contains three unknowns: k_1^*, k_2^*, and k_3^*. The number of unknowns can be reduced by imposing a certain distribution to the stiffness terms along the building height. Here, we force the stiffness distribution along the building height to be proportional to storey shear distribution, so that a uniform inter-storey drift profile is expected. The global stiffness terms become:

$$k_3^* = \frac{z_3 \cdot m_3}{\sum_{i=1}^{3}(z_i \cdot m_i)} k_1^*. \quad k_2^* = \frac{z_2 \cdot m_2 + z_3 \cdot m_3}{\sum_{i=1}^{3}(z_i \cdot m_i)} k_1^*. \quad k_1^* = \frac{z_1 \cdot m_1 + z_2 \cdot m_2 + z_3 \cdot m_3}{\sum_{i=1}^{3}(z_i \cdot m_i)} k_1^* = k_1^*. \quad (7)$$

where z_i and m_i represent the mass and the height of the i^{th} storey level, respectively.

Also, by replacing k_1^*, k_2^*, and k_3^* with their equivalent expressions in Eq. (7), and by doing some mathematical manipulation, the global stiffness becomes as follows:

$$\left[K^*\right]=\begin{pmatrix} 1+\frac{z_2 \cdot m_2 + z_3 \cdot m_3}{\sum_{i=1}^{3}(z_i \cdot m_i)} & -\frac{(z_2 \cdot m_2 + z_3 \cdot m_3)}{\sum_{i=1}^{3}(z_i \cdot m_i)} & 0 \\ -\frac{(z_2 \cdot m_2 + z_3 \cdot m_3)}{\sum_{i=1}^{3}(z_i \cdot m_i)} & \frac{z_2 \cdot m_2 + 2(z_3 \cdot m_3)}{\sum_{i=1}^{3}(z_i \cdot m_i)} & -\frac{z_3 \cdot m_3}{\sum_{i=1}^{3}(z_i \cdot m_i)} \\ 0 & -\frac{z_3 \cdot m_3}{\sum_{i=1}^{3}(z_i \cdot m_i)} & \frac{z_3 \cdot m_3}{\sum_{i=1}^{3}(z_i \cdot m_i)} \end{pmatrix} k_1^*. \quad (8)$$

The expression given in Eq. (8) shows that the global stiffness matrix is now dependent on only one term (k_1^*). As for the first iteration, it is possible to set k_1^* equal to k_1. Alternatively, k_1^* can be kept unknown, which makes the method non-iterative; however, the modal analysis would be very complicated when dealing with more than 3-DOFs having an unknown stiffness matrix.

3.2 Step 2: Modal analysis

A modal analysis of the controlled system is performed using the initial global stiffness and the mass matrices of the system. The modal analysis allows obtaining the elastic displacements at each storey and for the different modes, which are then combined using the SRSS rule given in Eq. (9). Afterwards, the inter-storey drifts at different storey levels are computed using Eq. (10),

$$u_i = \sqrt{\sum_{n=1}^{N}\left(u_{i,n}^2\right)}. \tag{9}$$

$$\delta_{ij} = \left|u_j - u_i\right|. \tag{10}$$

where u_i and u_j are the displacements at storeys i and j respectively, δ_{ij} is the storey drift between two successive storey levels i and j, n is the mode's number, N is the number of modes.

3.3 Step 3: Matching the design drifts

To fulfil the predefined design objective, the actual and the design inter-storey drifts should match. If the two drifts show a difference, the global stiffness matrix of the system is adjusted by adding an increment, as shown in Eq. (11), and the modal analysis is run again. This increment is given in Eq. (12). It should be noted that either Eq. (5) or Eq. (8) can be used for updating stiffness; however, if the latter is used, only k_1^* is updated because Eq. (8) is expressed in terms of k_1^*. Moreover, it is worth to note that the design drift of the structure must be equal or lower than its yielding drift because as we are performing a linear analysis, we are assuming that the behaviour of the structure is pure linear.

$$k_{i,r+1}^* = k_{i,r}^* \cdot C_{i,r} \tag{11}$$

$$C_{i,r} = 1 + \frac{a_{d,i,r} - d_{d,i,r}}{d_{d,i,r}} \geq 1. \tag{12}$$

where i is the storey number, r is the iteration number, C is the modification coefficient, a_d is the actual drift (obtained from the modal analysis $a_d = \delta$), d_d is the design drift (obtained from the predefined performance objectives).

3.4 Step 4: Stiffness of the CSB system

The target stiffness matrix of the bracing system is obtained by subtracting the stiffness matrix of the uncontrolled structure from the global stiffness matrix that we reach in the final iteration of step 3. The equation is given as follows:

$$\left[K_b\right] = \left[K^*\right] - \left[K\right] = \begin{pmatrix} k_{b1}+k_{b2} & -k_{b2} & 0 \\ -k_{b2} & k_{b2}+k_{b3} & -k_{b3} \\ 0 & -k_{b3} & k_{b3} \end{pmatrix}. \tag{13}$$

3.5 Step 5: Stiffness of the single CSB device:

At each storey level, the target stiffness of each CSB device is obtained by dividing the target stiffness components of the CSB system (k_{b1}, k_{b2} or k_{b3}) over the number of devices at that storey level, as in Eq. (14). The number of devices may be assigned by the professional designer in accordance with the architectural constraints in the building structure.

$$K_{CSB,i} = K_{b,i} / N_{CSB,i}. \tag{14}$$

where $K_{CSB,i}$ is the stiffness of the single CSB device at the i^{th} storey, $N_{CSB,i}$ is the number of devices at the i^{th} storey.

3.6 Step 6: Moment of inertia and cross section profile

The moment of inertia of each device is computed using the formulas introduced in Eqs. (1) and (2), where $\overline{K}$ is set equal to $K_{CSB,i}$, and $\overline{F}$ is the target yield strength at which we want the device to go inelastic. Once the moment of inertia is secured, the cross section profile can be picked from a broad range of cross sections. It is worth to note that the cross-section profile choice may control the post yielding behaviour of the bracing device, which in turn affects the post yielding behaviour of the whole structure. Therefore, different cross-section profiles should be tested so the inelastic performance objectives (i.e. PO corresponds to very rare EQ level) can be met.

4 NUMERICAL EXAMPLE

4.1 Case study structure

The case study structure is a new building located in Gubbio city, Italy. Gubbio is a city located in the far north-eastern part of the Italian province of Perugia, a relatively high seismic zone. The building is designed, and yet to be executed, to meet operational and life safety seismic objectives under occasional (SLD) and rare (SLV) earthquake levels respectively, according to the Italian building code [13]. As shown in Fig. 5, the planar geometry of the building structure is rectangular with dimensions equal to 34.11m x 19.10m. It is made up of two storey levels with 4.1m height each. The backbone forming the structure consists of three bays in the y-direction (Elevation 1) and two bays in the x-direction (Elevation 2).

The structure is composed of beams supported on columns, forming a moment-resisting frame system. The columns on the ground floor have a cross section of 60cm x 60cm, while the columns on the first floor have a cross section of 50cm x 50cm. The beams that form the main frames have rectangular cross sections with 40cm width and 50cm depth. Beams and columns are built adopting concrete C45/55 (average cubic strength R_{ck} equal to 55 MPa) and a modulus of elasticity $E=36000MPa$, which was reduced by half to take into account the inertia reduction due to crack formation, according to suggestions made by FEMA [14] and the Italian Building Code [13]. As for reinforcement bars, steel B540C (yield strength is equal to 450 MPa) is adopted.

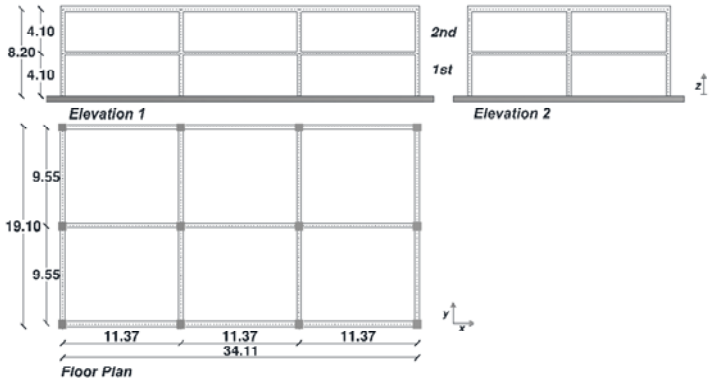

Figure 5- Elevations and plan of the studied building

4.2 The seismic input

In this work, two types of non-linear analysis are performed; static pushover analysis, which delivers the capacity curve of the structure starting from rest until the failure point [15], and

dynamic time-history analysis, which was conducted by scaling a set of seven accelerograms to the four design values of PGA, as indicated in Table 1, where T_y is the return period of the design earthquake, *PGA* is the peak ground acceleration, F_0 is the maximum spectral dynamic amplification, T_c^* is the characteristic period at the beginning of the constant velocity branch of the design spectrum. The ground motions are obtained using the software *SIMQKE_GR* [16] in such a way to be compatible with the design spectra at the fundamental period of the structure indicated by the Italian Building Code [13].

Table 1: Earthquake design levels with corresponding response spectra parameters

Earthquake design level	Earthquake performance level	$T_r[years]$	$PGA\,[g]$	F_0	$T_c^*[s]$
EQ1: frequent	Fully operational-SLO	30	0.071	2.391	0.270
EQ2: occasional	Damage-SLD	50	0.093	2.343	0.276
EQ3: rare	Life safety-SLV	475	0.230	2.392	0.310
EQ4: very rare	Near collapse-SLC	975	0.293	1.275	0.320

4.3 CSB bracing system

4.3.1 Performance objectives

The case study structure has been designed according to the Italian building code [13], thus it meets the "basic objectives" corresponding to the two earthquake design levels, occasional and rare, indicated in Fig. 1 and Table 1. For the sake of this study, higher requirements are set to be achieved by the structure. That is, the bracing system is installed in the structure to improve its seismic performance to meet the "essential objectives" specified in Fig. 1. Essential objectives require the structure to stay in a fully operational condition under occasional earthquake design level (EQ-2), to stay in an operational condition with limited yielding and damages under rare earthquake design level (EQ-3), and to have some degree of damage while preventing any life loss under very rare earthquake design level (EQ-4).

Performance objectives are usually set depending on the client's requirements, building' destination, building's importance, and building's typology [17]. Bertero et al. have proposed applicable performance limits based on structural and non-structural damage criteria, such as structural damage indexes (DM), storey drift indexes (IDI), and rate of deformations (floor velocity, acceleration) [1]. Those performance objectives, however, correspond to the basic objectives (Fig. 1); thus, they cannot be used in our design because our desire is to meet higher requirements. Table 2 shows the basic objectives corresponding to each of the four earthquake levels, as proposed by Bertero et al. (2002), and another set of performance limits belonging to the essential performance objectives, proposed by the authors. First, the inter-storey drift index (IDI) that corresponds to EQ-3 (PO-3) is set to be 0.005, which limits the damage of the non-structural components and prevents the yielding of the structural ones. Other objectives (PO-1, PO-2, and PO-4) were selected proportionally to the ground motions at the fundamental period of the structure.

Table 2: Quantification of the basic and the essential performance objectives

Limit state	IDI [1] (Basic objectives)	Limit state	IDI (Essential objectives)
EQ1: Fully operational	0.003	EQ1: Fully operational	PO-1 = 0.0015
EQ2: Damage	0.006	EQ2: Fully operational	PO-2 = 0.0020
EQ3: Life safety	0.015	EQ3: Damage	PO-3 = 0.0050
EQ4: Near collapse	0.020	EQ4: Life safety	PO-4 = 0.0067

4.3.2 Design of the CSB devices (x-direction)

Step 1: Global stiffness matrix

$$[M]=\begin{pmatrix} m_1 & 0 \\ 0 & m_2 \end{pmatrix}=\begin{pmatrix} 8781.55 & 0 \\ 0 & 7035.165 \end{pmatrix}(kN)$$

$$[K]=\begin{pmatrix} 338474+163230 & -163230 \\ -163230 & 163230 \end{pmatrix}(\frac{kN}{m})$$

$$[K^*]=\begin{pmatrix} 1+\frac{z_2\cdot m_2}{\sum_{i=1}^{2}(z_i\cdot m_i)} & -\frac{z_2\cdot m_2}{\sum_{i=1}^{2}(z_i\cdot m_i)} \\ -\frac{z_2\cdot m_2}{\sum_{i=1}^{2}(z_i\cdot m_i)} & \frac{z_2\cdot m_2}{\sum_{i=1}^{2}(z_i\cdot m_i)} \end{pmatrix}.k_1^*$$

$$=\begin{pmatrix} 1+0.615 & -0.615 \\ -0.615 & 0.615 \end{pmatrix}.k_1(\frac{kN}{m})$$

Step 2: Modal analysis (SLV response spectrum)

Inter-storey drifts:

$\delta_{01}=2.63cm$

$\delta_{12}=3.46cm$

Step 3: Matching the design drifts

Design drifts:

$\delta_{01,d}=0.005.h=0.005*410=2.05cm$

$\delta_{12,d}=0.005.h=0.005*410=2.05cm$

Global stiffness matrix at the final iteration:

$$[K^*]=\begin{pmatrix} 826650 & -312290 \\ -312290 & 312290 \end{pmatrix}(\frac{kN}{m})$$

Step 4: Stiffness of the CSB system

$$[K_b]=[K^*]-[K]=\begin{pmatrix} 324950 & -149060 \\ -149060 & 149060 \end{pmatrix}(\frac{kN}{m})$$

$k_{b1}=175890\frac{kN}{m}$

$k_{b2}=149060\frac{kN}{m}$

Step 5: Stiffness of the single CSB device

Structural configuration:

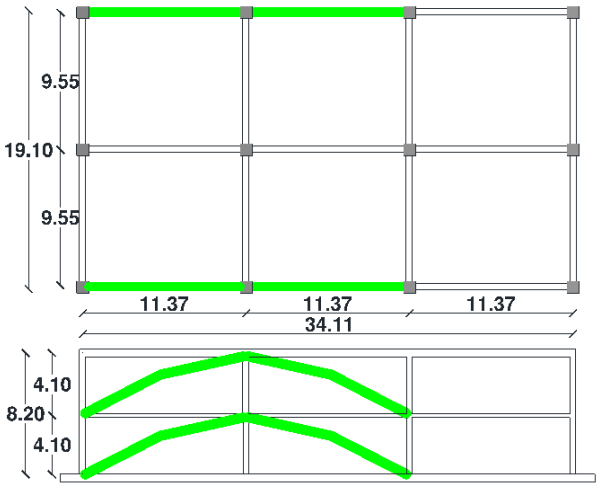

$N_{CSB,1}=N_{CSB,2}=4$

$k_{CSB,1}=\frac{175890}{4}=43972.5\frac{kN}{m}$

$k_{CSB,2}=\frac{149060}{4}=37265\frac{kN}{m}$

Step 6: Moment of inertia and cross section profile

Arm ratio: $\xi=0.1$

Moments of inertia:

$J_1=139684.3\ cm^4 \qquad J_2=118377\ cm^4$

Cross sections:

$CSB_1:\ rectangular\ \ 48cm\times 15cm$

$CSB_2:\ rectangular\ \ 45cm\times 15cm$

4.4 Numerical verification

In this section, we aim at verifying the achievement of the pre-defined seismic performance objectives through a numerical simulation of the seismic behaviour of the case study structure. For this purpose, a finite element model has been developed using the commercial software SAP2000 [18]. The constitutive law of the CSB bracing elements was obtained using the fibre-based software 'SeismoStruct V.7.0.6' [10], and then inserted in SAP2000 as non-linear links (NL).

Pushover analysis is first conducted using two displacement shapes (linear and uniform), whose average is considered. The base shear and the roof (top) displacement have been used to represent the force and displacement, respectively. Fig. 6(a) shows the capacity spectra of the controlled and uncontrolled buildings and the essential performance objectives in S_{ad} format. Investigation of the graph shows that the capacity curve of the controlled structure matches exactly the predefined target curve. On the other hand, the capacity spectrum of the uncontrolled structure was unable to fulfil the predefined seismic performances.

Another type of analysis, non-linear time-history analysis, has been performed to evaluate the seismic performance of the structure. Four groups of spectrum-compatible accelerograms have been considered in agreement with the EQ levels reported in Table 1. Each group consists of seven ground motion records scaled to the PGA of the corresponding EQ level at the fundamental period of the structure. The results of the time-history analyses are plotted in Fig. 6(b), where each point represents the maximum base shear and ultimate displacement of the corresponding time-history analysis. Investigation of the graph allows observing that the seismic response of the uncontrolled structure fails to achieve the predefined performances, unlike the controlled structure whose time-history analyses results show a large agreement with the prescribed objectives.

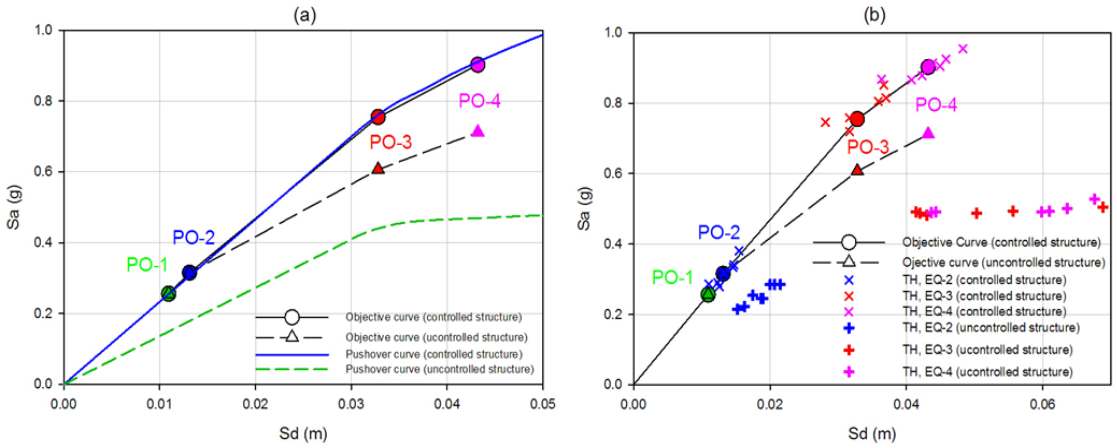

Figure 6- (a) Acceleration-displacement capacity spectra of the controlled and uncontrolled structures with the performance objectives. (b) Time-history response of the controlled and uncontrolled structures with the performance objectives

5 CONCLUSIONS

In this paper, a comprehensive procedure for the seismic design of a multi-storey frame structure equipped with energy dissipation Crescent Shaped Brace devices within the performance-based seismic design (PBSD) is proposed. CSBs have a special geometrical configuration that allows the structure to meet different pre-selected seismic performances. The design procedure composes of six steps and is based on the modal analysis.

A two-story reinforced concrete structure equipped with crescent-shaped braces (CSB) is analysed to verify the validity of the proposed method. First, the seismic objectives are set. Performance objectives are expressed in terms of the storey drift index (IDI), which is an indicator of the non-structural damage. Once the objectives are known, the CSB devices are designed accordingly using the proposed design procedure. The studied structure is then subjected to static pushover and dynamic time-history analyses, whose results are plotted using the S_{ad} format. The results demonstrate a good agreement between the capacity curve and the objective curve of the controlled structure. All four pre-selected seismic performances corresponding to different seismic levels have been perfectly met.

It is worth to note that all previous attempts concerning the design of CSB focused on SDOF structures. This design procedure, however, can be applied to both SDOF and MDOF shear-type structures. For other types of structures, more investigations are currently undergoing.

ACKNOWLEDGEMENTS

The research leading to these results has received funding from the European Research Council under the Grant Agreement n° ERC_IDEal reSCUE_637842 of the project IDEAL RESCUE— Integrated DEsign and control of Sustainable CommUnities during Emergencies.

Financial supports of Department of Civil Protection (DPC-RELUIS 2014-2018 Grant – Research line 6 "Seismic isolation and dissipation", WP2: "Energy dissipation", Task 2.6: "Definizione di metodi di progetto, procedure e software dedicati ai sistemi di dissipazione di energia e proposte di normativa sviluppate nell'ambito del presente progetto") is gratefully acknowledged.

REFERENCES

[1] Bertero, D. B. Raul, and V. Vitelmo. "Performance-based seismic engineering: the need for a reliable conceptual comprehensive approach," *Earthquake Engineering & Structural Dynamics,* vol. 31, pp. 627-652, 2002.

[2] Özuygur and A. Ruzi. "Performance-based Seismic Design of an Irregular Tall Building — A Case Study," *Structures,* vol. 5, pp. 112-122, 2016.

[3] B. S. Taranath. "Seismic Rehabilitation of Existing Buildings," in *Wind and Earthquake Resistant Buildings*, ed: CRC Press, pp. 499-584, 2004.

[4] M. Palermo, I. Ricci, S. Gagliardi, S. Silvestri, T. Trombetti, and G. Gasparini. "Multi-performance seismic design through an enhanced first-storey isolation system," *Engineering Structures,* vol. 59, pp. 495-506, 2014.

[5] T. Hoang, K. T. Ducharme, Y. Kim, and P. Okumus. "Structural impact mitigation of bridge piers using tuned mass damper," *Engineering Structures,* vol. 112, pp. 287-294, 4/1/ 2016.

[6] T. K. Datta. "Seismic Control of Structures," in *Seismic Analysis of Structures*, ed: John Wiley & Sons, Ltd, pp. 369-449, 2010.

[7] Chopra and K. Anil. *Dynamics of structures : theory and applications to earthquake engineering*. Upper Saddle River, N.J.: Prentice-Hall, 2001.

[8] M. Palermo, S. Silvestri, G. Gasparini, and T. Trombetti. "Crescent shaped braces for the seismic design of building structures," *Materials and Structures,* vol. 48, pp. 1485-1502, 2014.

[9] S. V. Committee. "Performance-based seismic engineering. ," Report prepared by Structural Engineers Association of California, Sacramento, CA, 1995.

[10] SeismoStruct. "Seismosoft Earthquake Engineering Software Solutions," ed.

[11] A. Correia and F. Virtuoso. "Nonlinear analysis of space frames," in *Proceedings of the third European conference on computational mechanics: solids, structures and coupled problems in engineering*, Lisbon, 2006.

[12] F. Filippou, E. Popov, and V. Bertero. "Effects of bond deterioration on hysteretic behavior of reinforced concrete joints," Earthquake Engineering Research Center, University of California, Berkeley1983.
[13] NTC. "Norme Tecniche per le Costruzioni, Italian building code, adopted with D.M. 14/01/2008, published on S.O. no. 30 G.U. no. 29 04/02/2008.
[14] F. E. M. A. 356. "Seismic Rehabilitation Guidelines," 2000.
[15] T. K. Datta, "Inelastic Seismic Response of Structures," in *Seismic Analysis of Structures*, ed: John Wiley & Sons, Ltd, pp. 237-274, 2010.
[16] E. H. Vanmarcke, C. A. Cornell, D. A. Gasparini, and S. Hou. "SIMQKE_GR ", ed, 1990.
[17] I. Ricci, S. Gagliardi, G. Gasparini, S. Silvestri, T. Trombetti, and M. Palermo. "First-Storey Isolation Concept for Multi-Performance Seismic Design of Steel Buildings," in *15 WCEE*, LISBOA, 2012.
[18] I. Computers and Structures. "SAP2000," 18.1 ed, 2015.